

Two-dimensional cellular automaton model of traffic flow with open boundaries

Shin-ichi Tadaki*

Department of Information Science, Saga University, Saga 840, Japan

(Received 5 February 1996)

A two-dimensional cellular automaton model of traffic flow with open boundaries are investigated by computer simulations. The outflow of cars from the system and the average velocity are investigated. The time sequences of the outflow and average velocity have flicker noises in a jamming phase. The low-density behaviors are discussed with simple jam-free approximations. [S1063-651X(96)02609-8]

PACS number(s): 64.60.Cn, 05.70.Ln

I. INTRODUCTION

Models of traffic flow have relations to wide varieties of physical systems. A traffic flow system is one of the asymmetric exclusion processes. They are nontrivial statistical mechanical systems because of a lack of detailed balance. Studies of these nontrivial systems explore the profound structure of statistical mechanics. Studies of exclusively interacting particle systems, like traffic flow, also relate to equilibrium and nonequilibrium properties of granular flows, surface growth, dynamics of defects in solids, and so on. The model I will discuss here may be one of the simplest examples of nonequilibrium colliding granular flows.

Traffic flow problems have been studied mainly through fluid dynamics, car-following models, coupled map lattice models, and cellular automaton (CA) models. Many attempts have been made to apply CA modeling to complex phenomena including fluid because of computational simplicity. Cellular automaton modeling of traffic flow is one of the recently developing areas. One of the simplest CA models of traffic flow in a one-way expressway is the rule-184 elementary CA [1], which is a simple asymmetric exclusion rule. In spite of the simplicity of the model, it shows a phase transition from a freely moving phase at low vehicle density to a jamming phase at high vehicle density. The computational simplicity of CA models also enables us to take many realistic features of traffic problems into account. More realistic models considering speed variation of cars or effects of blockades have been investigated in one-dimensional models [2–5]. $1/f$ fluctuation has been observed in both actual expressways [6] and models [3,7]. Self-organized criticality has also been studied [8].

Traffic networks, for example, a traffic system of a whole city or an expressway network, consist of many complicated ingredients. It is very hard to model all of the features of traffic networks. Two-dimensional CA models of traffic flow, therefore, are very abstract models of traffic networks. One of the simplest two-dimensional CA models of traffic flow has been investigated by Biham, Middleton, and Levine (BML) [9]. Their model is a simple extension of the rule-184 CA to two dimension. Cars are distributed on a square lattice of $N \times N$ sites with periodic boundaries both in the horizontal

and vertical directions. They found a sharp transition between a freely moving phase at low vehicle density and a jamming phase at high vehicle density. The characteristics of the transition were studied by Nagatani [10] and Fukui and Ishibashi [11,12]. Two types of jam phase were discussed by Tadaki and Kikuchi [13,14]. The model has been extended to take into account the probability of changes in vehicle directions [15,16].

Two-dimensional CA models of traffic flow show many physically interesting phenomena, phase transitions, and self-organization. Cellular automaton modeling of traffic systems, however, is a toy model. It should be clarified which features strongly depend on the model itself. Characteristic features of the BML model are, for example, deterministic dynamics, periodic boundaries, restrictions on the car destination, road arrangement without traffic queue [17], and so on. In this paper, open boundary conditions instead of periodic ones are used to investigate the emergence of a traffic jam in a two-dimensional CA model.

The organization of this paper is as follows: The model is given in Sec. II. The dynamics is described with binary arrays. The outflow of cars from the system is investigated in Sec. III. The jam-free approximation is discussed. In Sec. IV the average velocity of cars is investigated. Section V is devoted to discussions.

II. MODEL

The model is the same as model I of BML except for the boundary conditions. Contrary to the original BML model, cars are injected probabilistically into both the left and lower boundaries of the system and flow out deterministically from both the right and upper boundaries.

Up-directed and right-directed cars are exclusively distributed in the $N \times N$ square lattice. Each site is empty or occupied by one up-directed or right-directed car. Cars can move one step at a time if and only if the adjacent site in the destination is empty. There is a traffic light controlling the whole system as up-directed cars can move only at even time steps and right-directed cars only at odd time steps.

The number of right-directed (up-directed) cars at a time t and a position $\vec{r} = (i, j)$ ($1 \leq i, j \leq N$) is expressed by a binary array $\mu_{\vec{r}}(t) = \{0, 1\}$ [$\nu_{\vec{r}}(t) = \{0, 1\}$] [16]. The bulk dynamics, namely, dynamics for bulk sites (i, j) ($1 \leq i \leq N$, $1 < j < N$ for up-directed and $1 < i < N$, $1 \leq j \leq N$ for right-

* Electronic address: tadaki@ai.is.saga-u.ac.jp

directed cars) can be expressed as

$$\begin{aligned}\mu_{\vec{r}}(t+1) &= \sigma(t)\mu_{\vec{r}}(t)\{\mu_{\vec{r}+\vec{x}}(t) + \nu_{\vec{r}+\vec{x}}(t)\} \\ &+ \sigma(t)\{1 - \mu_{\vec{r}}(t)\}\{1 - \nu_{\vec{r}}(t)\}\mu_{\vec{r}-\vec{x}}(t) \\ &+ \{1 - \sigma(t)\}\mu_{\vec{r}}(t),\end{aligned}\quad (1)$$

$$\begin{aligned}\nu_{\vec{r}}(t+1) &= \{1 - \sigma(t)\}\nu_{\vec{r}}(t)\{\mu_{\vec{r}+\vec{y}}(t) + \nu_{\vec{r}+\vec{y}}(t)\} \\ &+ \{1 - \sigma(t)\}\{1 - \mu_{\vec{r}}(t)\}\{1 - \nu_{\vec{r}}(t)\}\mu_{\vec{r}-\vec{y}}(t) \\ &+ \sigma(t)\nu_{\vec{r}}(t),\end{aligned}\quad (2)$$

where \vec{x} and \vec{y} denote unit vectors of right and up directions, respectively. The binary function $\sigma(t) = t \bmod 2$ represents the control by the traffic light. The condition $\mu_{\vec{r}}(t)\nu_{\vec{r}}(t) = 0$ holds because one site can not be occupied by both up and right cars simultaneously.

The first term $\sigma(t)\mu_{\vec{r}}(t)\{\mu_{\vec{r}+\vec{x}}(t) + \nu_{\vec{r}+\vec{x}}(t)\}$ in Eq. (1) denotes that a right-directed car remains at the site \vec{r} if the right adjacent site is occupied by a right-directed or up-directed car. The injection of a right-directed car from the left adjacent site is given by the second term $\sigma(t)\{1 - \mu_{\vec{r}}(t)\}\{1 - \nu_{\vec{r}}(t)\}\mu_{\vec{r}-\vec{x}}(t)$. The last term $\{1 - \sigma(t)\}\mu_{\vec{r}}(t)$ shows that a right-directed car does not move at odd time steps. The same decomposition of Eq. (2) can be done for the dynamics of up-directed cars.

Cars are injected from the lower and left sides of the system. If the site on the edges of the system is empty, a car is injected with a probability p . The injection of right-directed cars on the left edge $\vec{r} = (1, j)$ ($1 \leq j \leq N$) is given by replacing the injection term (second term) in Eq. (1) with a probabilistic injection

$$\begin{aligned}\mu_{\vec{r}}(t+1) &= \sigma(t)\mu_{\vec{r}}(t)\{\mu_{\vec{r}+\vec{x}}(t) + \nu_{\vec{r}+\vec{x}}(t)\} \\ &+ \sigma(t)\{1 - \mu_{\vec{r}}(t)\}\{1 - \nu_{\vec{r}}(t)\}f(p) \\ &+ \{1 - \sigma(t)\}\mu_{\vec{r}}(t),\end{aligned}\quad (3)$$

where $f(p) = \{0, 1\}$ is a function which returns unity with a probability p . The injection of up-directed cars on the lower edge $\vec{r} = (i, 1)$ ($1 \leq i \leq N$) is given by

$$\begin{aligned}\nu_{\vec{r}}(t+1) &= \{1 - \sigma(t)\}\nu_{\vec{r}}(t)\{\mu_{\vec{r}+\vec{y}}(t) + \nu_{\vec{r}+\vec{y}}(t)\} \\ &+ \{1 - \sigma(t)\}\{1 - \mu_{\vec{r}}(t)\}\{1 - \nu_{\vec{r}}(t)\}f(p) \\ &+ \sigma(t)\nu_{\vec{r}}(t).\end{aligned}\quad (4)$$

Cars flow out from the upper and right edges of the system deterministically. The dynamical equations for cars on the upper and right edge are given by deleting the first terms in Eqs. (1) and (2). For sites on the right edge $\vec{r} = (N, j)$ ($1 \leq j \leq N$),

$$\begin{aligned}\mu_{\vec{r}}(t+1) &= \sigma(t)\{1 - \mu_{\vec{r}}(t)\}\{1 - \nu_{\vec{r}}(t)\}\mu_{\vec{r}-\vec{x}}(t) \\ &+ \{1 - \sigma(t)\}\mu_{\vec{r}}(t)\end{aligned}\quad (5)$$

gives the dynamics of right-directed cars on the right edge. For sites on the upper edge $\vec{r} = (i, N)$ ($1 \leq i \leq N$),

100×100($p=0.40$)



FIG. 1. A snapshot of the simulation. The system size is 100×100 and $p = 0.4$. The black and gray dots show right-directed and up-directed cars, respectively. There are some local jam clusters. Jam clusters are sorted out with the maximum throughput ($\rho = 2/3$).

$$\begin{aligned}\nu_{\vec{r}}(t+1) &= \{1 - \sigma(t)\}\{1 - \mu_{\vec{r}}(t)\}\{1 - \nu_{\vec{r}}(t)\}\nu_{\vec{r}-\vec{y}}(t) \\ &+ \sigma(t)\nu_{\vec{r}}(t)\end{aligned}\quad (6)$$

gives the dynamics of up-directed cars on the upper edge.

In the current simulations, the system has no car at the initial time $t = 0$. Cars are injected with Eqs. (3) and (4) probabilistically and run deterministically obeying Eqs. (1) and (2). If cars reach the edges of the system, they flow out by Eqs. (5) and (6). In the early traffic light cycles $O(N)$, the front lines of right-directed and up-directed cars collide to form a global traffic jam configuration in case $p > p_c$ (p_c is discussed later). The global jam is sorted out with the maximum throughput, where the number of cars per site is $\rho = 2/3$. Then new small jam clusters are created and sorted out again and again. Figure 1 shows a snapshot of the system. In the simulation, the system runs $200N$ times ($100N$ traffic light cycles) from the initial condition for relaxation and quantities discussed later are observed for $200N < t \leq 400N$.

III. OUTFLOW

The first quantity we observe is the outflow of cars from the system. By virtue of the dynamics, Eqs. (5) and (6), the outflow is the number of cars appearing on the upper and right edges of the system. The average outflow \bar{p}_{out} is defined as the average number of cars appearing on the edges per site and traffic light cycle. The results of the simulation are given in Fig. 2.

In the low injection p region, the system can be assumed to be free from a traffic jam. In this case the injection process will be controlled only by the number of cars which stay on the lower and left edges of the system. The number of up-directed (right-directed) cars in each column (row) is given by $\bar{p}_{\text{out}}N$. There are $2\bar{p}_{\text{out}}N$ cars on the left edge of the system. These cars prevent car injection from the left side of the system, and the remaining $(1 - 2\bar{p}_{\text{out}})N$ sites can accept car injection. At the next time step, therefore, the number of cars injected on the left edge will be $(1 - 2\bar{p}_{\text{out}})Np$. The equilibrium condition between the injection and the outflow

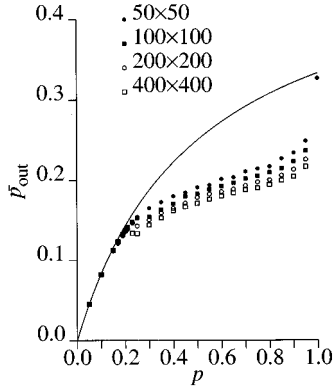


FIG. 2. Average outflow from the system for the system size 50×50 , 100×100 , 200×200 , and 400×400 . The bold line gives the jam-free approximation $\bar{p}_{\text{out}} = p/(1+2p)$, which is given in the text.

$$\bar{p}_{\text{out}} = (1 - 2\bar{p}_{\text{out}})p \quad (7)$$

gives

$$\bar{p}_{\text{out}} = \frac{p}{1+2p} \quad (8)$$

as the average outflow. This naive estimation of the outflow (jam-free approximation) agrees well with the simulation results for $p < p_c$ ($p_c \sim 0.2$). The extrapolation of Eq. (8) to $p = 1$ gives $\bar{p}_{\text{out}} = 1/3$, which corresponds to the maximum throughput.

In the high injection p region, the system has traffic jam clusters in the bulk area. The outflow \bar{p}_{out} is suppressed and lower than that given by the jam-free approximation discussed above.

The time-dependent behavior of the outflow $p_{\text{out}}(t')$ (t' denotes the traffic light cycle and $t' = 0, \dots, T-1$) and its power spectrum

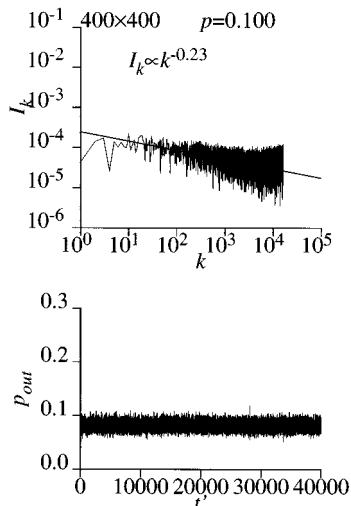


FIG. 3. Time-dependent behavior of $p_{\text{out}}(t)$ for $p=0.1$ with the system size 400×400 and its power spectrum I_k . The bold line is fitted with the power spectrum $10^1 < k < 10^3$ by the method of least squares.

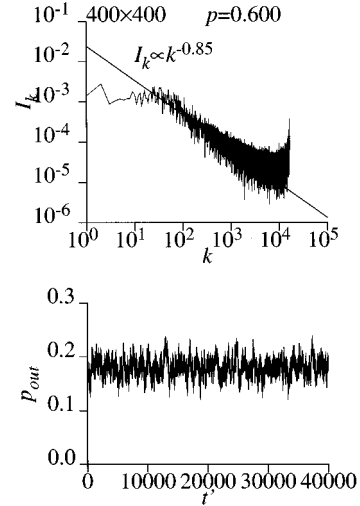


FIG. 4. Time-dependent behavior of $p_{\text{out}}(t)$ for $p=0.6$ with the system size 400×400 and its power spectrum I_k . The bold line is fitted with the power spectrum $10^1 < k < 10^3$ by the method of least squares.

$$I_k = \left| \frac{1}{T} \sum_{t'=0}^{T-1} p_{\text{out}}(t') e^{-2\pi i k t' / T} \right|^2 \quad (9)$$

is observed, where T is the maximum traffic light cycles obeying $T = 2^7 < 100N$ [18]. In the high p region (Fig. 4), the power spectrum of $p_{\text{out}}(t)$ shows $I_k \sim k^{-\alpha}$ behavior (Fig. 5). This shows the existence of the self-organized jam clusters in the bulk system. In the low p region (Fig. 3), on the other hand, $p_{\text{out}}(t')$ shows random fluctuation around the average and the power spectrum is beared with weak flicker noise.

IV. AVERAGE VELOCITY

The average velocity of the cars is the number of cars moving during one traffic light cycle (namely, two time steps). The arrays μ and ν are binary ones. Thus the average velocity, is half of the Hamming distance between $\mu(t)$ and $\mu(t+2)$ [$\nu(t)$ and $\nu(t+2)$]. Caution must be paid to tread

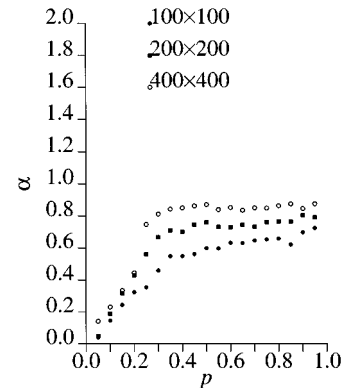


FIG. 5. The behavior of the exponent α . The exponents are calculated to fit the power spectrum I_k within $10^1 < k < 10^3$ with the method of least squares. In the high $p > p_c$ region, the exponent behaves as a constant $\alpha \sim 0.8$ which depends on the system size. Below the critical p_c the exponent sharply decreases because the low p power spectrum shows a weak flicker noise.

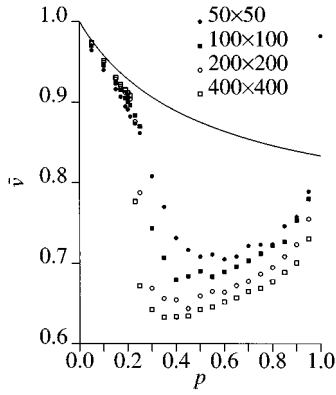


FIG. 6. Average velocity for the system size 50×50 , 100×100 , 200×200 , and 400×400 . The bold line is $\bar{v} = 1 - (1/2)p/(1+2p)$.

the edges of the system. For example, for right-directed cars, if the left edge site is empty the site must be excluded from the calculation of the Hamming distance because of the probabilistic injection. If the right edge site is occupied by right-directed car, the site must be excluded because of the deterministic outflow. The same treatment is applied to up-directed cars. Figure 6 shows the results of the simulation.

In the low p region, the jam-free approximation gives the outflow \bar{p}_{out} as discussed in Sec. III. There are $2\bar{p}_{\text{out}}N^2$ cars in the system. Assuming no jam in the bulk area, cars are distributed randomly. There are $\bar{p}_{\text{out}}^2N^2$ colliding pairs of cars. The number of freely moving cars will be $2\bar{p}_{\text{out}}N^2(1 - (1/2)\bar{p}_{\text{out}})$. And the average velocity is

$$\bar{v} = 1 - \frac{1}{2} \frac{p}{1+2p}. \quad (10)$$

This estimation agrees with the results of the simulation less than the case of the outflow. The discrepancy seems to come from the effect of collisions with more than two cars. These effects are expected to decrease faster than two-car collisions in large systems. The simulation results seem to show that the jam-free approximation becomes better with increasing system size.

At the critical injection $p_c \sim 0.2$, the average velocity shows a sharp phase transition with its sudden decrement by the formation of jam clusters. It increases gradually with the increment of p above p_c . The behavior of \bar{v} just above p_c shows strong finite size effects.

The time-dependent average velocity $v(t')$ and its power spectrum

$$J_k = \left| \frac{1}{T} \sum_{t'=0}^{T-1} v(t') e^{-2\pi i k t' / T} \right|. \quad (11)$$

shows the same characteristics as those of the outflow (Figs. 7 and 8). The high p case shows the flicker noise as $J_k \sim k^{-\beta}$ with $\beta \sim 1.2$ (Fig. 9) reflecting the emergence of a traffic jam. The low p average velocity seems to have weak flicker noises. This shows the temporary formation of a small traffic jam.

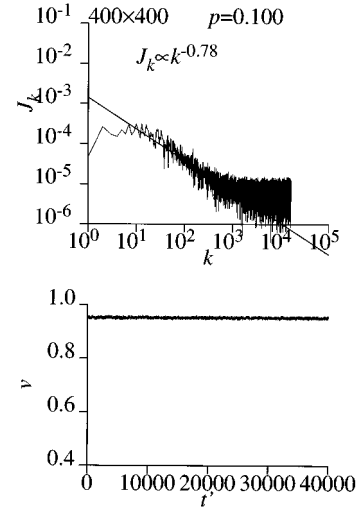


FIG. 7. Time-dependent behavior of $v(t)$ for $p=0.1$ with the system size 400×400 and its power spectrum J_k . The bold line is fitted with the power spectrum $10^1 < k < 10^3$ by the method of least squares.

V. DISCUSSION

In this paper a two-dimensional cellular automaton traffic flow model with open boundaries was investigated by computer simulation. The bulk dynamics is deterministic. Cars are probabilistically injected from the left and lower sides of the system and flow out from the right and upper sides deterministically.

The average outflow \bar{p}_{out} , which is the number of cars flowing out from the right and upper sides per traffic light cycle and per site, obeys $\bar{p}_{\text{out}} = p/(1+2p)$ in the low injection region ($p < p_c$), where p is the injection rate. This is well understood with the jam-free approximation. High injection $p > p_c$ causes the emergence of traffic jam clusters in the system and suppress the outflow. In the high injection

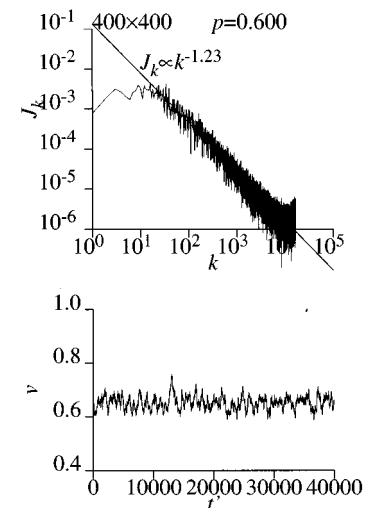


FIG. 8. Time-dependent behavior of $v(t)$ for $p=0.6$ with the system size 400×400 and its power spectrum J_k . The bold line is fitted with the power spectrum $10^1 < k < 10^3$ by the method of least squares.

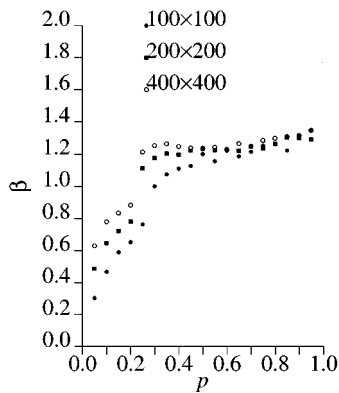


FIG. 9. The behavior of the exponent β . The exponents are calculated to fit the power spectrum J_k within $10^1 < k < 10^3$ with the method of least squares. In the high $p > p_c$ region, the exponent behaves as a constant $\beta \sim 1.2$ which depends on the system size. Below the critical p_c the exponent sharply decrease because the low p power spectrum shows a weak flicker noise.

region, the time-dependent behavior of the outflow shows flicker noises.

The average velocity of cars was also investigated. The jam-free approximation value $\bar{v} = 1 - p/(1 + 2p)/2$ does not agree well with the simulation results. The reason seems to be the many car collision effect which will be suppressed in a large system size. The average velocity shows sharp phase transition at $p_c \sim 0.2$. In the high injection region, the average velocity is suppressed by the emergence of traffic jam clusters. The time-dependent behavior of the average velocity also shows flicker noises in the high injection region. In the low injection region, it shows weak flicker noise because of the formation of temporal jam clusters.

In the original BML model, which has periodic boundaries, cars are freely moving with $\bar{v} = 1$ in the low density region. On the contrary, the current system with open boundaries shows the average velocity less than unity even in the jam-free state. The reason for the difference is as follows: As is well known in a one-dimensional case (Wolfram's rule-184), temporal jam clusters in the low density region are sorted out and form the maximum throughput current with

the local density $\rho = 1/2$. Sorting out of jam clusters gives the average velocity $\bar{v} = 1$. In two-dimensional cases, temporal jam clusters are also sorted out and form the maximum throughput current with $\rho = 2/3$. In the periodic boundary cases, once the *coherent* maximum throughput currents are created, they dominate the whole system and new traffic jam clusters are hardly created. In the open boundary cases, on the other hand, the *coherent* maximum throughput currents flow out from the system and the *incoherent* currents are injected. These *incoherent* injections form new traffic jam clusters and suppress the average velocity.

In this paper, I called the event at $p \sim 0.2$ *phase transition*. The event is not a phase transition in the strictest sense of the word. No critical behavior is found at that point. The value of the average velocity shows sharp discontinuity at $p \sim 0.2$. It has finite value above the point however. An adequate order parameter is needed to strictly define the phase transition.

In Fig. 6, the average velocity increases above the point $p \sim 0.4$. As mentioned above, the maximum flow with $\rho = 2/3$ is formed behind jam clusters. The contribution of the maximum flow to the average velocity is expected to grow with the injection rate p . The increment of p also seems to enhance the deterministic feature of the injection process. These factors may contribute to the increment of the average velocity. On the contrary, the increment of the injection rate p contributes to the formation of jam clusters which decreases the average velocity. The competition of this cluster formation effect and the previous two factors decides the behavior of the average velocity. The investigations of the statistical and dynamical properties of spatial structures may clarify the behavior of the system.

Tadaki and Kikuchi show the existence of two types of jam phases in the BML model [13,14]. The current models with open boundaries, seems to have only one jam phase. The high density random jam phase found in the periodic boundary case seems to be one of the finite size effects. In the viewpoint of statistical mechanics, finite size effects will be neglected in realistic macroscopic systems. On the contrary, real traffic network systems are finite and the finiteness may be an important factor of the system. Observations of real traffic network systems are expected.

-
- [1] S. Wolfram, Rev. Mod. Phys. **55**, 601 (1983).
 [2] K. Nagel and M. Schreckenberg, J. Phys. I (France) **2**, 2221 (1992).
 [3] K. Nagel and H. J. Herrmann, Physica A **199**, 254 (1993).
 [4] A. Schadschneider and M. Schreckenberg, J. Phys. A **26**, L679 (1993).
 [5] S. Yukawa, M. Kikuchi, and S. Tadaki, J. Phys. Soc. Jpn. **63**, 3609 (1994).
 [6] T. Musha and H. Higuchi, Jpn. J. Appl. Phys. **15**, 1271 (1976).
 [7] M. Takayasu and H. Takayasu, Fractals **1**, 860 (1993).
 [8] K. Nagel and M. Paczuski, Phys. Rev. E **51**, 2909 (1995).
 [9] O. Biham, A. A. Middleton, and D. Levine, Phys. Rev. A **46**, 6124 (1992).
 [10] T. Nagatani, J. Phys. Soc. Jpn. **62**, 2625 (1993).
 [11] M. Fukui and Y. Ishibashi, J. Phys. Soc. Jpn. **62**, 3841 (1993).
 [12] Y. Ishibashi and M. Fukui, J. Phys. Soc. Jpn. **63**, 2822 (1994).
 [13] S. Tadaki and M. Kikuchi, Phys. Rev. E **50**, 4564 (1994).
 [14] S. Tadaki and M. Kikuchi, J. Phys. Soc. Jpn. **64**, 4504 (1995).
 [15] J. A. Cuesta, F. C. Martínez, J. A. Molera, and A. Sánchez, Phys. Rev. E **48**, 5175 (1993).
 [16] J. A. Molera, F. C. Martínez, J. A. Cuesta, and R. Brito, Phys. Rev. E **51**, 175 (1995).
 [17] J. Freund and T. Pöschel, Physica A **219**, 95 (1995).
 [18] The fast Fourier transform is carried with the FORTRAN subroutine named TFTR (D6/CTU0078F/TFTR) created by Keiia Takakubo and registered in the Computer Center, Tohoku University.